

# Wave-train Induced Unpinning of Weakly Anchored Vortices in Excitable Media

Alain Pumir<sup>1,2</sup>, Sitabhra Sinha<sup>3</sup>, S. Sridhar<sup>3</sup>, M  d  ric Argentina<sup>2</sup>, Marcel H  rning<sup>4</sup>,  
Simonetta Filippi<sup>5</sup>, Christian Cherubini<sup>5</sup>, Stefan Luther<sup>6</sup> and Valentin Krinsky<sup>6,7</sup>

<sup>1</sup>*Laboratoire de Physique, ENS de Lyon and CNRS, 46 All  e d'Italie, 69007, Lyon, France.*

<sup>2</sup>*Lab J. A. Dieudonn  , Universit   de Nice and CNRS, Parc Valrose, F-06108 Nice Cedex, France.*

<sup>3</sup>*The Institute of Mathematical Sciences, CIT Campus, Taramani, Chennai 600113, India.*

<sup>4</sup>*Dept. of Physics, Graduate School of Science, Kyoto University, Kyoto 606-8502, Japan.*

<sup>5</sup>*Nonlinear Physics & Math Modeling Lab, University Campus Bio-Medico, I-00128, Rome, Italy.*

<sup>6</sup>*MPI for Dynamics and Self-Organization, Am Fassberg 17, D-37077, G  ttingen, Germany. and*

<sup>7</sup>*Institut Non Lin  aire de Nice and CNRS, F-06560, Valbonne, France.*

(Dated: June 7, 2010)

A free vortex in excitable media can be displaced and removed by a wave-train. However, simple physical arguments suggest that vortices anchored to large inexcitable obstacles cannot be removed similarly. We show that unpinning of vortices attached to obstacles smaller than the core radius of the free vortex is possible through pacing. The wave-train frequency necessary for unpinning increases with the obstacle size and we present a geometric explanation of this dependence. Our model-independent results suggest that decreasing excitability of the medium can facilitate pacing-induced removal of vortices in cardiac tissue.

PACS numbers: 87.19.Hh, 05.45.-a, 87.19.lp, 05.45.Gg

Rotating spiral waves of propagating excitation characterize the disruption of ordered behavior in excitable media describing a broad class of physical, chemical and biological systems [1]. In the heart, spiral waves of electrical activity have been associated with life-threatening arrhythmias [2–4], i.e., breakdown of the normal rhythmic pumping action of the heart. Controlling such spatial patterns with low-amplitude external perturbation is a problem of fundamental interest [5–9] with significant implications for the clinical treatment of cardiac arrhythmias [10].

In a homogeneous active medium, a spiral wave can be controlled by a wave train, induced by periodic stimulation from a local source (pacing)[4]. If the frequency of stimulation is higher than that of the spiral wave, the wave train induces the spiral to drift. In a finite medium, the vortex is eventually driven to the boundary and thereby eliminated from the system [11–13]. Inhomogeneities in the medium, such as inexcitable obstacles, can anchor the spiral wave preventing its removal by a stimulated wave-train [14]. This mechanism is analogous to pinning of vortices in disordered superconductors [15, 16]. In the heart, obstacles such as blood vessels or scar tissue, can play the role of pinning centres [17], leading to anatomical reentry, the sustained periodic excitation of the region around the obstacle.

In the immediate neighborhood of the obstacle, pinned vortices are qualitatively equivalent to waves circulating in a one-dimensional ring. They can be removed by external stimulation provided the electrode is located on the reentrant circuit, i.e., the closed path of the vortex around the obstacle, and the stimulus is delivered within a narrow time interval [18]. However, for the more general situation of pacing waves generated far away from the reentrant circuit, a classical result due to Wiener

and Rosenblueth (WR) states that, all waves circulating around such obstacles are created or annihilated in pairs (see Ref. [19], in particular, pp.216-224). This implies that it is impossible to unpin the spiral wave by a stimulated wave train.

In this paper, we demonstrate that the WR mechanism for the failure of pacing in unpinning spiral waves is valid only when the radius of the *free* spiral core (i.e., the closed trajectory of the spiral tip defined as a phase singularity [20]) is small compared to the size of the obstacle. We elucidate the transition between the case of a free vortex and one attached to a large obstacle by systematically decreasing the core radius of the free spiral,  $R_{FS}$ , relative to the obstacle size,  $R_{obst}$ , by increasing the excitability of the medium. Our main result is that an anchored rotating wave can be removed by a stimulated wave train provided  $R_{FS} > R_{obst}$ .

To illustrate our arguments, we use the simple model of excitable media introduced in Ref. [21], described by an excitatory ( $u$ ) and a recovery ( $v$ ) variable:

$$\begin{aligned}\partial_t u &= \frac{1}{\epsilon} u(1-u)[u - (v + \frac{b}{a})] + \nabla^2 u, \\ \partial_t v &= (u - v),\end{aligned}\tag{1}$$

where,  $a$  and  $b$  are parameters describing the kinetics. The relative time-scale  $\epsilon$  between the local dynamics of  $u$  and  $v$  is set to 0.02. We discretize the system on a square spatial grid of size  $L \times L$ , with a lattice spacing of  $\Delta x = 0.25$  and time step of  $\Delta t = 0.01$ . For our simulations  $L = 200$ . We solve Eq. 1 using forward Euler scheme with a standard nine-point stencil for the Laplacian. No flux boundary conditions are implemented at the edges of the simulation domain. An obstacle is implemented by introducing a circular region of radius  $R_{obst}$  in the center of simulation domain inside which diffusion

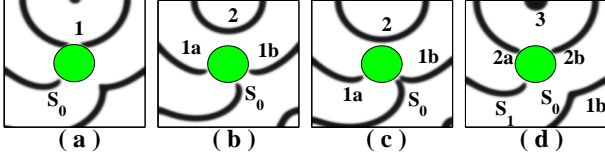


FIG. 1: (a) Wave  $S_0$ , pinned to an obstacle (shaded), rotates counterclockwise; wave 1 is the first pacing wave. (b) Wave 1 hits the obstacle, and separates into a wave rotating counterclockwise (1a) and a wave rotating clockwise (1b). (c) Waves  $S_0$  and 1b collide and merge leaving only one rotating wave 1a denoted  $S_1$  hereafter. (d) The wave resulting from the merging of  $S_0$  and 1b leaves the system. The interaction between the following pacing wave, 2 and  $S_1$ , is similar to that shown in (a-c). Thus, the pinned vortex persists. Numerical simulation of the Barkley model with parameters:  $a = 0.9$ ,  $b = 0.17$ ; the pacing period is  $T_p = 6.7$  and the radius of the obstacle is  $R = 6.5$ .

is absent. Pacing is delivered by setting the value of  $u$  to  $u_p = 0.9$  in a region of  $6 \times 3$  points at the center of the upper boundary of the simulation domain. The maximum pacing frequency is limited by the *refractory period*,  $T_{ref}$ , the duration for which stimulation of an excited region does not induce a response.

When the obstacle size is large relative to the core radius of the free spiral,  $R_{FS}$ , the failure of a wave train in unpinning the vortex is illustrated in Fig. 1. Initially, the spiral wave  $S_0$  rotates counterclockwise around the obstacle. During the interaction with pacing waves, the number of waves attached to the obstacle can change due to two possible processes (see Ref. [19], p.216 and 220). First, when the pacing wave reaches the obstacle, it splits into two oppositely rotating waves: one clockwise and the other counterclockwise. Second, collision between two rotating waves, as seen in Fig. 1(c), results in the annihilation of a pair of counterclockwise and clockwise waves. In both cases, the number of waves rotating counterclockwise is always larger than the number rotating clockwise by 1. Thus, in addition to conservation of total topological charge (i.e., sum of the individual chiralities, +1 or -1) for *all* spiral waves in a medium [20, 22], topological charge *around* the obstacle also appears to be conserved. However, in the limiting case of infinitesimally small obstacle corresponding to a free vortex, a stimulated wave-train with frequency higher than that of the spiral wave will always succeed in displacing the latter, eventually removing it from a finite medium. Thus, there is a transition from failure to successful pacing as  $R_{obst}$  is reduced relative to  $R_{FS}$ .

The primary fact responsible for this transition is that the spiral wave is no longer in physical contact with an obstacle of size smaller than  $R_{FS}$  [17], contrary to the fundamental assumption of Ref. [19]. Fig. 2 shows an explicit example of successful detachment of a pinned wave from the obstacle boundary, where the core radius

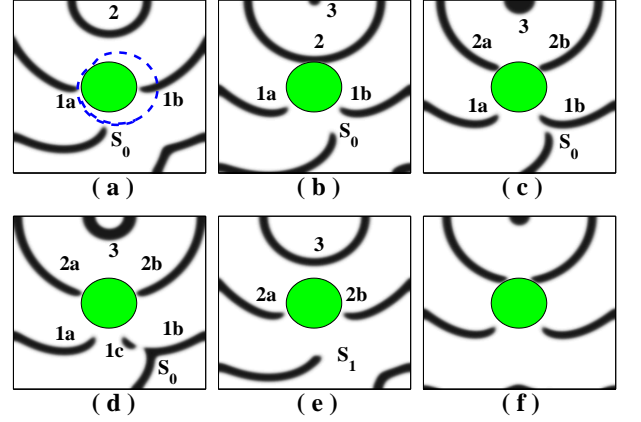


FIG. 2: Lowering excitability results in successful detachment of pinned vortex by pacing.  $S_0$  is a rotating wave whose core (dashed line) is larger than the pinning center (shaded). (a-c) are topologically as in Fig. 1. (d) A wavelet 1c is produced after collision of waves  $S_0$  and 1b, in contrast with Fig. 1(d). (e) The wavelet 1c collides with 1a and the resulting wave  $S_1$  is displaced away from the obstacle. (f) Subsequent pacing induces drift of the spiral wave  $S_1$  to the boundary, eventually removing it from the medium. The parameters are as in Fig. 1, except for  $a = 0.895$  and  $b = 0.1725$ , resulting in increasing the vortex core size.

of a free spiral in the medium is made larger than  $R_{obst}$  by diminishing the excitability of the system.

The possibility of unpinning the wave in Fig. 2 can be traced to the following fact: the collision between  $S_0$  and the pacing wave-branch 1b occurs a *small distance away* from the obstacle boundary and does not result in complete annihilation of both waves. A small fragment 1c survives in the spatial interval between the collision point and the obstacle [Fig. 2(d)]. If the tip of  $S_0$  is close to the obstacle, the fragment 1c is small, and rapidly shrinks and disappears. However, if the gap between the reentrant wave tip and the obstacle is large at the collision point, such that the size of 1c is larger than a critical value  $l_n$ , the fragment can survive. As 1c propagates further away, it collides with the pacing wave 1a and forms a new broken wave  $S_1$  that is completely detached from the obstacle. Interaction with successive pacing waves progressively pushes the vortex further away from the obstacle, and eventually from a finite medium. The difference between the number of spirals rotating counterclockwise and clockwise *around the obstacle* changes from 1 initially (Fig. 2, a), to 0 in Fig. 2(e), contrary to what happens for a larger obstacle (Fig. 1). The absence of topological charge conservation for waves rotating *around* a smaller obstacle underlines the breakdown of the fundamental assumption behind the WR argument for why pacing cannot detach pinned waves. The unpinned wave is subsequently driven outside the system boundaries by

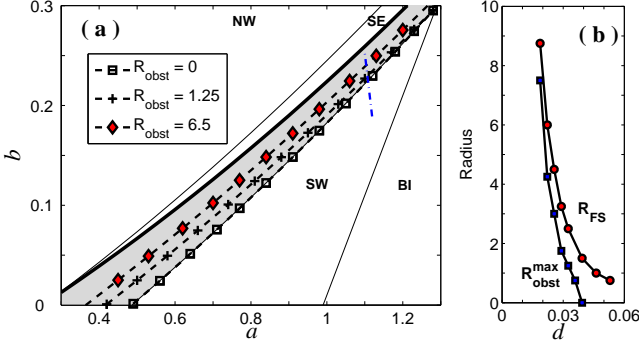


FIG. 3: (a) Parameter space of the Barkley model. Unpinning is possible in the shaded portion of the SW region, which exhibits persistent spiral waves. The thick line indicates the boundary with the SE region, where spirals cannot form. The domain where unpinning is possible shrinks with increasing size of the pinning center, the three dashed lines corresponding to  $R_{obst} = 0$ , i.e., no obstacle (square),  $R_{obst} = 1.25$  (plus) and  $R_{obst} = 6.5$  (diamond). (b) Radius  $R_{FS}$  of the free spiral and the maximum obstacle radius  $R_{obst}^{max}$  from which wave trains can unpin vortices, as a function of the distance  $d$  from the SE-SW boundary, along the dot-dashed line indicated in (a). Note that  $R_{FS} > R_{obst}^{max}$ , and both increase with decreasing  $d$ . [In (a), NW (BI) indicates the parameters for which steady waves are absent (the medium is bistable).]

pacing (Fig. 2, f), thus eventually also reducing the total topological charge of the *finite* medium to 0.

The relative size of the obstacle, compared to the free spiral core, is the key parameter that decides whether a pinned reentrant wave can be removed or not. Indeed, the radius of the free spiral core in the successful case,  $R_{FS} = 9.05$  (Fig. 2) is significantly larger than in the unsuccessful one,  $R_{FS} = 5.80$  (Fig. 1). It is further confirmed by a detailed numerical study of the interaction between a pacing wave train and a pinned spiral over the  $(a, b)$  parameter space of the Barkley model. As shown in Fig. 3(a), the rotating wave anchored to the obstacle can be removed by pacing only in the neighborhood of the sub-excitable (SE) region (using the terminology of Ref. [23]), where  $R_{FS}$  diverges [Fig. 3(b)]. This is explained by noting that in the SE regime, the tangential velocity of a broken wavefront is negative, thus causing the front to shrink and not form a spiral. As we approach the regime where spiral waves are persistent (SW), the tangential velocity of the wave break gradually increases to zero and becomes positive on crossing the SE-SW boundary, so that the broken wave front can now evolve into a spiral. As  $R_{FS}$  increases with decreasing tangential velocity of the wave front, the spiral core becomes large close to the SE region resulting in successful pacing-induced termination of pinned reentry.

We observe that there is a maximum radius of the obstacle ( $R_{obst}^{max}$ ) close to  $R_{FS}$  above which pacing is unsuccessful in detaching the anchored spiral wave [Fig. 3(b)].

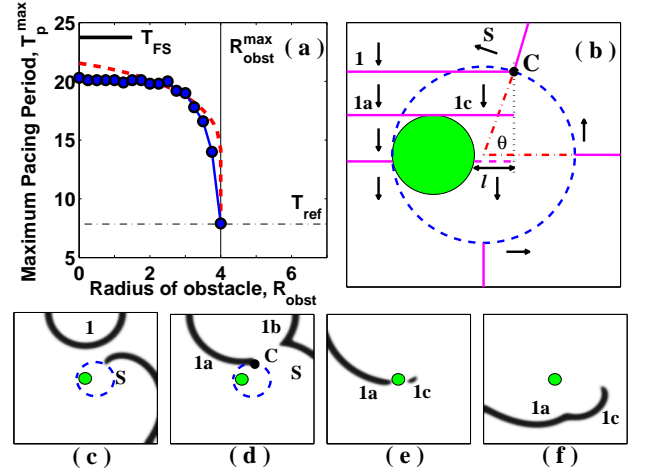


FIG. 4: (a) The maximum pacing period  $T_p^{max}$  at which unpinning is possible as a function of the obstacle radius  $R_{obst}$ . For the parameters  $a = 1.1323$ ,  $b = 0.2459$  that we have used, the maximum radius of obstacle from which depinning can occur is  $R_{obst}^{max} = 4$ .  $T_{FS}$  is period of a free spiral wave and  $T_{ref}$  is the refractory period. The dashed line indicates the prediction from Eq. 2. (b) The wavelet formation mechanism leading to the detachment of the pinned vortex (schematic). (c-f) Numerical simulation of the Barkley model.  $S$  collides with wave 1 at point  $C$  at an angle  $\theta$ . The part 1b of the pacing wave merges with  $S$ , moving out of the system. The remaining part of the pacing wave collides with the obstacle (shaded) separating into 1a and a small wavelet 1c. When the length  $l$  of wavelet 1c is larger than the critical nucleation length, 1c survives and collides with  $S$ . This results in unpinning of  $S$ .

Fig. 4(a) shows that the pacing period for successful unpinning from the obstacle is bounded by the refractory period ( $T_{ref}$ ) and a maximum value  $T_p^{max}$  that is independent of  $R_{obst}$  for small obstacles. As we approach  $R_{obst}^{max}$ , the upper bound sharply decreases, becoming equal to the refractory time at  $R_{obst}^{max}$ , which indicates that pacing will be unsuccessful in unpinning waves attached to obstacles of radii larger than  $R_{obst}^{max}$ . Thus, the results shown in Figs. 3(b) and 4(a) demonstrate our earlier assertion that pacing induced removal of anchored waves will be possible only when the obstacle is smaller than the core radius of the free spiral wave in the medium.

Our numerical results indicate that the maximum pacing period necessary for detaching a pinned spiral wave is a decreasing function of the obstacle size [Fig. 4(a)]. This can be explained semi-quantitatively by the following geometric argument, valid when the size of the obstacle is small compared to the core size of the spiral, and supported by the simulations shown in Fig. 4(c-f). The tip of the spiral  $S$  moves along its circular trajectory, shown by the broken line in Fig. 4(b), and interacts with the pacing wave coming from the top, represented by a solid line. The part 1b of the pacing wave collides with  $S$  at the point  $C$  characterized by an angle  $\theta$  that the spiral

tip makes with the symmetry axis (i.e., the line joining the centers of the obstacle and spiral core); the resulting wave eventually leaves the system [Fig. 4(d)]. The remaining section of the pacing wave splits into two waves,  $1a$  and  $1c$ , propagating along either side of the obstacle. The wave tip moves approximately in a straight line from  $C$ , so that the length of the wave  $1c$  at the symmetry axis is  $l = R_{FS}(1 + \cos \theta) - 2R_{obst}$ . When the fragment  $1c$  is larger than the nucleation size  $l_n$ , it expands into a wavefront that reconnects with wave  $1a$ . This results in a displacement of the wave  $1a$  away from the obstacle, leading to unpinning (as in Fig. 2). For  $l < l_n$ ,  $1c$  shrinks and eventually disappears, resulting in unsuccessful pacing.

Thus, the condition for detachment is  $l \geq l_n$ . The length  $l$  is a decreasing function of the angle  $\theta$ , which in turn, is a decreasing function of the pacing period,  $T_p$ , as explained below. The relation between  $T_p$  and  $\theta$  can be established by estimating the time interval for two successive collisions of the spiral with the pacing waves. From the point of collision  $C$ , the pacing wave reaches the obstacle after time  $T_1 = (R_{FS} \sin \theta - R_{obst})/v$ , and the symmetry axis after time  $T_2 = T_1 + (R_{obst}T_{FS}/4R_{FS})$ . From the symmetry axis, the new reentrant wave  $S$  moves by an angle  $(\theta + \pi)$  to arrive at  $C$  at time  $T_3 = T_2 + [T_{FS}(\theta + \pi)/2\pi]$ , where it collides with the next pacing wave. Noting that  $T_3 = T_p$  allows us to implicitly express  $T_p$  as a function of  $\theta$ , and thereby,  $l$ . The maximum pacing period leading to detachment is obtained when  $l = l_n$ , as:

$$T_p^{max} = \frac{R_{FS}}{v}(\sin \theta_c - f_R) + \frac{f_R T_{FS}}{4} + \frac{T_{FS}(\theta_c + \pi)}{2\pi}, \quad (2)$$

where,  $\theta_c = \arccos(2f_R - 1 + [l_n/R_{FS}])$  and  $f_R = R_{obst}/R_{FS}$ . When  $R_{obst} > R_{obst}^{max} = R_{FS} - (l_n/2)$ ,  $T_p^{max}$  has complex values, indicating that for larger obstacles the fragment is too small to survive. The nucleation length  $l_n$  can thus be estimated from  $R_{obst}^{max}$ , which allows us, in turn, to determine the dependence of  $T_p^{max}$  as a function of  $R_{obst}$  from Eq. 2. Fig. 4(a) shows this to be in fair agreement with our numerical simulations.

We stress that the arguments used here are model independent, and are based only on the property that waves in excitable media annihilate on collision. We verified numerically that wave-train induced unpinning is observed also in a more detailed and realistic description of cardiac tissue, the Luo-Rudy model [24] [see the movie on line], under conditions of reduced excitability. Meandering, which occurs in the Barkley model at low  $a, b$  values (Fig. 3, a), does not affect the physical effect discussed here. Note that the proposed unpinning mechanism is for the case of an obstacle smaller than the vortex core. It is possible under certain circumstances to unpin waves from obstacles larger than the core because of other effects such as the presence of slow conduction regions [25] and nonlinear wave propagation (alternans) [26].

Our results thus predict that in cardiac tissue, the removal of spiral waves pinned to a small obstacle by high-frequency wave trains is facilitated by decreasing the excitability of the medium. This is consistent with previous experimental results on cardiac preparations using Na-channel blockers [17] and our prediction could be directly tested in a similar experimental setup [12, 17].

In conclusion, we have shown that for a pinned vortex interacting with a pacing wave train, unpinning is possible when the size of the obstacle is smaller than that of the spiral core. The minimum wave train frequency necessary for unpinning in the presence of an inexcitable obstacle is higher than that for inducing drift in a free vortex towards the boundaries, and it increases with the size of the pinning center. Our results suggest that lowering the excitability of the medium makes it easier to unpin vortices by pacing.

This research was initiated at the Kavli Institute for Theoretical Physics, and was supported in part by IFCPAR (Project 3404-4) and IMSc Complex Systems Project (XI Plan).

- 
- [1] M. C. Cross and P. C. Hohenberg, Rev. Mod. Phys. **65**, (1993).
  - [2] V. I. Krinsky, Vestnik A.N. SSSR 1-12 (1980).
  - [3] J. M. Davidenko *et al.*, Nature (London) **355**, 349 (1992).
  - [4] *Cardiac Electrophysiology: From Cell to Bedside*, edited by D. P. Zipes and J. Jalife (Saunders, Philadelphia, 2004).
  - [5] S. Sinha, A. Pande, and R. Pandit, Phys. Rev. Lett. **86**, 3678 (2001);
  - [6] S. Takagi *et al.*, Phys. Rev. Lett. **93**, 058101 (2004).
  - [7] H. Zhang *et al.*, Phys. Rev. Lett. **94**, 188301 (2005).
  - [8] S. Sinha and S. Sridhar, in *Handbook of Chaos Control* (2nd edition, Wiley-VCH, Weinheim, 2008), p. 703; S. Sridhar and S. Sinha, EPL **81**, 50002 (2008).
  - [9] A. Isomura *et al.*, Phys. Rev. E **78**, 066216 (2008); M. Hörning *et al.*, Phys. Rev. E **79**, 026218 (2009).
  - [10] F. Fenton *et al.*, Circulation **120**, 467 (2009).
  - [11] V. Krinsky and K. Agladze, Physica D **8**, 50 (1983).
  - [12] K. Agladze *et al.*, Am. J. Physiol. Heart Circ. Physiol. **293**, H503 (2007).
  - [13] G. Gottwald *et al.*, Chaos **11**, 487 (2001).
  - [14] A. M. Pertsov *et al.*, Physica D **14**, 117 (1984); M. Vinson *et al.*, Physica D **72**, 119 (1994); Z. A. Jimenez *et al.*, Phys. Rev. Lett. **102**, 244101 (2009); B. T. Ginn *et al.*, Phys. Rev. Lett. **93**, 158301 (2004).
  - [15] G. Blatter *et al.*, Rev. Mod. Phys. **66**, 1125 (1994).
  - [16] D. Pazo *et al.*, Phys. Rev. Lett. **93**, 168303 (2004).
  - [17] Z. Y. Lim *et al.*, Circulation **114**, 2113 (2006).
  - [18] L. Glass and M. E. Josephson, Phys. Rev. Lett. **75**, 2059 (1995).
  - [19] N. Wiener and A. Rosenblueth, Arch. Inst. Cardiol. Mexico, **16**, 205 (1946).
  - [20] A. T. Winfree, *When Time Breaks Down*, Princeton Univ Press, Princeton NJ (1987).
  - [21] D. Barkley *et al.*, Phys. Rev. A **42**, 2489 (1990).

- [22] L. Glass, *Science* **198**, 321 (1977).
- [23] S. Alonso *et al.*, *Science* **299**, 1722 (2003).
- [24] C. H. Luo and Y. Rudy, *Circ. Res.* **68**, 1501 (1991).
- [25] S. Sinha *et al.*, *Chaos* **12**, 893 (2002); S. Sinha and D.J. Christini, *Phys. Rev. E* **66**, 061903 (2002).
- [26] J. Breuer and S. Sinha, *Pramana* **64**, 553 (2005).